Mapping Amazon Basin Wetlands through Region Growing Segmentation and Unsupervised Region Classification of JERS-1 Data

Cláudio Barbosa[1], Laura Hess[2], John Melack[2], Evlyn Novo[1], Mary Gastil[2], and Luciano Dutra[1]
[1]*Remote Sensing Division, National Institute for Space Research, C.P. 515, CEP 12201-970, São José dos Campos, Brazil.*
[2]*Institute for Computational Earth System Science, University of California, Santa Barbara, CA, 93106, USA*

ABSTRACT: A methodology is described for mapping the Amazon Basin Wetlands using region growing segmentation and region classification of multi-date JERS-1 data. The proposed methodology includes the following steps: imagery segmentation, feature extraction, unsupervised region classification, merging and mapping of unsupervised classes to three basic ones, editing, quality control through digital and visual revision, and, finally, addition to the basin mosaic.

1 INTRODUCTION

Wetlands comprise about 6% of the world's surface (Williams, 1991). Natural wetlands are a major source of atmospheric methane, a greenhouse gas that is increasing at an estimated annual rate of 1 per cent (Blake and Rowland 1986, Matthews and Fung 1987). The estimate of global carbon cycle and carbon and methane budgets must consider the wetland contribution. However a basic requirement is accurate quantitative information about wetland spatial distribution.

The annual average water level variation along the central Amazon river main stem of 7 to 13 meters leads to water penetrating inland 20 to 100 km, creating an enormous floodplain ecosystem (Goulding et al. 1995). In spite of its size and ecological importance, a geo-referenced map of the wetlands of the entire Amazon Basin is lacking. Several authors have mentioned this lack of information as a key problem for the regional studies regarding the carbon cycle (Junk, 1985; Piedade et al, 1991; Novo et al, 1997). Moreover, the application of sustainable development policies for the Amazon depends on a sound scientific understanding of the environment. Therefore, a sound knowledge of the functioning of Amazon Wetlands is mandatory.

The large extent and lack of accessibility of major floodplains make remote sensing the only practical method for monitoring inundation at the basin scale (Hess et al, 1995). The application of satellite optical sensors, such as the Landsat Thematic Mapper, is limited by tropical weather condition characterized by cloud cover.

As Synthetic Aperture Radar (SAR) systems are not limited by weather conditions and can detect flooding beneath many types of wetland vegetation (Hess et al, 1990), they have been used as an alternative source of data for land cover and wetland mapping.

The extraction of information from SAR images is usually a complex task, since SAR systems employ coherent radiation and the resulting images are corrupted by multiplicative signal-dependent noise known as speckle (Lucca et al, 1998). There are some methods to reduce speckle, e.g.; multi-look, filtering, etc (Oliver, 1998), but these methods cannot eliminate all the speckle. Several procedures have been adopted in the past to classify SAR data such as a decision-tree model (Hess et al, 1995.), maximum likelihood and an Iterated Conditional Modes (ICM) algorithm (Freitas 1998), and ICM classification of textural bands built by filtering polarimetric SIR-C data (Sant'ana 1998). Since single-frequency SAR have significant limitations (Hess et al, 1995), all these approaches were successfully applied to multi-frequency airborne SAR data and based on per-pixel classification.

The application of JERS-1 mosaic data to map the Amazon basin wetlands is not a simple task. The main difficulties are:

- Calibration problems within JERS-1 mosaic.
- Single frequency data.
- Data volume.

Costa et al. (1998) represents one successful attempt of mapping Amazon floodplain habitats using segmentation and supervised classification at Lago Grande in Monte Alegre region. Their best figures, however, were obtained with multi-date and multi-sensor data.

Images from two dates (low and high water) are the only data available for mapping the entire Amazon Basin wetlands.

So the purpose of this project was to propose a methodology for mapping the inundated Amazon Basin areas, using low and high water JERS-1 mosaics supplied by Jet Propulsion Laboratory (JPL). The experiment described in the next sections assesses the proposed methodology and presents results for a section of the Amazon Basin, near Manaus, used to develop and test the approach.

2 TEST SITE

A complex section of the JERS-1 mosaic (04° S to 00° S, 66° W to 60° W) near Manaus, was selected to develop the methodology (green hatched area in Figure 1). This area covers 297,400 km^2, and includes large areas of floodplain: varzea, which is flooded by sediment and nutrient-rich water (white water), and igapó, which is flooded by nutrient-poor water (black water) (Sioli, 1968). This area also includes a wide variety of vegetation typical of wetlands in the central Amazon Basin and therefore is ideal for performing the proposed study.

Figure 1 shows the entire area (magenta and orange) where wetlands shall eventually be mapped. Magenta (5,088,630 km^2) represents lowland Amazon basin (defined as areas less than 500 m in elevation). Orange (291,685 km^2) represents the Para and Amapa wetlands, outside the Amazon River Basin, but inside the Amazon region.

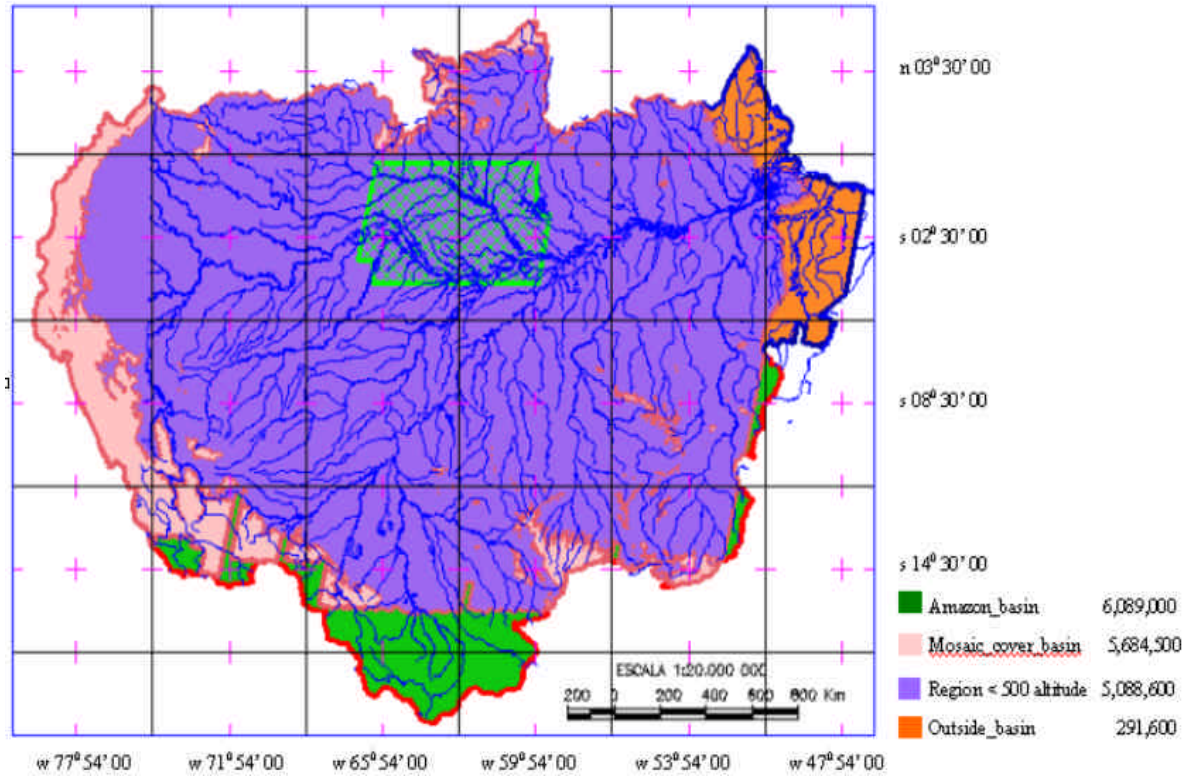

Figure 1 Test Area (green hatched) and the entire area to be mapped(magenta plus orange).

3 DATA AND METHODS

During September-November 1995 (low water) and May-June 1996 (high water) SAR images were acquired by the National Space Development Agency of Japan´s JERS-1 satellite (Hess et al., 1998). The JERS-1 scene calibration and the mosaicking were accomplished by JPL at Pasadena (Chapman et al., 2002).

DEM (Digital Elevation Model) data used to define lowland Amazon basin (altitude lower than 500 m) are available at http://edcwww.cr.usgs.gov/landdaac/gtopo30.

All image analyses were made using SPRING (Sistema de Processamento de Informacoes Georeferenciada), a freeware Geographical Information and Image Processing System with an object-oriented data model which provides for the integration of raster and vector data format in a single environment http://www.dpi.inpe.br/spring (Camara et al., 1996). The test site encompassed a JERS-1 3 arc-seconds pixel resolution (93m at the equator) of 4800 lines by 7200 columns or a 34 Mbytes file for each 8-bit image date.

The methodology includes the following steps: georeferencing, imagery segmentation, feature extraction, unsupervised region classification, merging and mapping of unsupervised classes to three basic ones, editing, quality control through digital and visual revision, and, finally, addition to the basin mosaic. Figure 2 shows these steps.

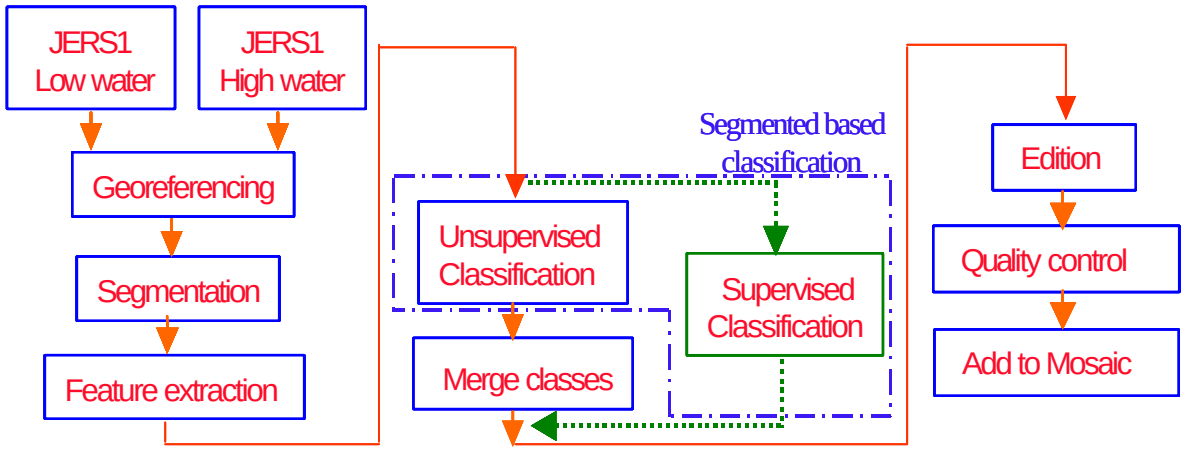

Figure 2 Steps of mapping (Flowchart)

(a) Georeferencing

High and low water JERS1 images were mosaicked, radiometrically calibrated and geo-referenced at the Jet Propulsion Laboratory. These mosaicked images from the test site were imported to the SPRING system, where the steps shown in Fig. 2 were carried out.

(b) Region growing segmentation

Pixel-based classification can result in a number of problems for SAR data due to the speckle noise (Lobo et al., 1996). To overcome these problems, the images were first submitted to a segmentation procedure. This procedure permitted running a region-based classification instead of pixel-based classification. Image segmentation is the process, by which individual image pixels are grouped into partitions, according to some intrinsic properties of the image, e.g., gray levels, contrast, spectral values or textural properties (Le Moigne and Tilton, 1995). The result of segmentation is a number of homogeneous regions, each having an unique label. There are several techniques to automatically segment digital images (Pal, 1993). The region growing technique is available in SPRING software. This technique is an iterative process by which regions are merged starting from individual pixels, growing iteratively until every pixel is processed and thereby forming regions whose boundaries are defined by closed polygons (Bins et al., 1996). To execute the segmentation, the user must provide two thresholds: similarity and minimum area. Similarity denotes the minimum difference in the gray level observed between two spatially adjacent pixels or average gray level of a set of pixels, which will yield different regions. If this difference is less than the similarity threshold value, the pixels belong to the same region. The minimum area threshold is associated with the smallest region size in pixels. In the segmented image, no region will be smaller than this threshold, defined by the user. Careful scrutiny and many trial-and-error interactions are required to establish these two thresholds. The appropriate values also depend on the data type and user needs. In this study, some critical areas over the entire image were selected and a study was made over these to define the best values. The segmentation process was carried out on images of two dates.

(c) Feature extraction

The aim of feature extraction phase is to determine the statistical attributes of each region outlined by one of the polygons resulting from the segmentation process. The result of the feature extraction phase is a file that contains a list of regions sorted in descending order according to their area. For each region on the list, the file also contains several statistics from the images selected by the user. In this study, two JERS1 images were selected on different dates. These statistical attributes may be used for a supervised or unsupervised classification; in both cases they will be used to determine the similarity measure between two regions outlined by polygons.

(d) Unsupervised Classification

An unsupervised classification based on a clustering algorithm was applied to the list of regions, characterized by their statistical attributes, defined in the feature extraction file. The clustering algorithm, named ISOSEG (Bins et al., 1992) uses the covariance matrix and mean vector of the regions to estimate the centers of the classes.

Roughly speaking, the classification process can be described by the following steps:

1. The user provides a percentage acceptance threshold. This threshold defines the maximum Mahalanobis distance (Richards, 1995) by which regions can be from the center of one class, and be considered as belonging to that class. It also determines the number of classes "clusters" detected by the algorithm.
2. The statistical attributes of the first region of the list (the largest one), are taken as the initial parameters of the first class. The classifier assumes that regions with large areas are the most representative of the class. Iteratively, the classifier removes from the list all regions with Mahalanobis distance smaller than the acceptance threshold.
3. Based on all regions removed from the list, a new center for the class is recalculated. This process is repeated until none of the regions are removed from the list. The next classes are recognized in the same way until the feature extraction list is emptied.
4. On the previous step, the regions were classified according to the order of cluster generation. This procedure may result in misclassification for some of the regions. To correct this possible distortion, the regions are reclassified using the new centers defined on the previous step.
5. If the number of classes after the reclassification procedure, step 4, is larger than the number defined on step 3, the algorithm uses the following approach to eliminate some classes: Classes with a small number of regions are eliminated, and regions from these classes are reclassified using the minimum Mahalanobis distance criterion.

The user controls the level of detail through the acceptance threshold: more classes for high significance levels (<80%) or less classes for low significance level (> 95%).

This region-based classification approach was successfully used by Batista et al. (1994) and Shimabukuro et al. (1998) to assess deforestation in the Amazon region.

(e) Merging of classes

This is an interactive phase where all resulting classes were reclassified into three classes, (flooded, non-flooded, open-water). The user defines the reclassification rules by comparing the high-low color composite and the classification results.

(f) Editing

It is generally accepted that visual interpretation provides better classification accuracy than machine classification, because the interpreter can use additional clues, such as area, shape and contextual information, including topographic information, results of previous classification, etc. A region-based classification, in which the algorithm uses some contextual attributes besides spectral values of the pixels, is an attempt to improve digital classification. Even this alternative can result in an inadequate classification, so the procedure reported here, similar to other techniques, requires editing after the digital analysis steps to eliminate misclassified set of pixels. The editing is accomplished through the identification, on the computer screen, of flooded areas that were misclassified. The identification is made by inspecting the display of the high-low color composite image overlapped with the classification results. Misclassified areas are outlined and merged to the correct class as shown in Figure 3.

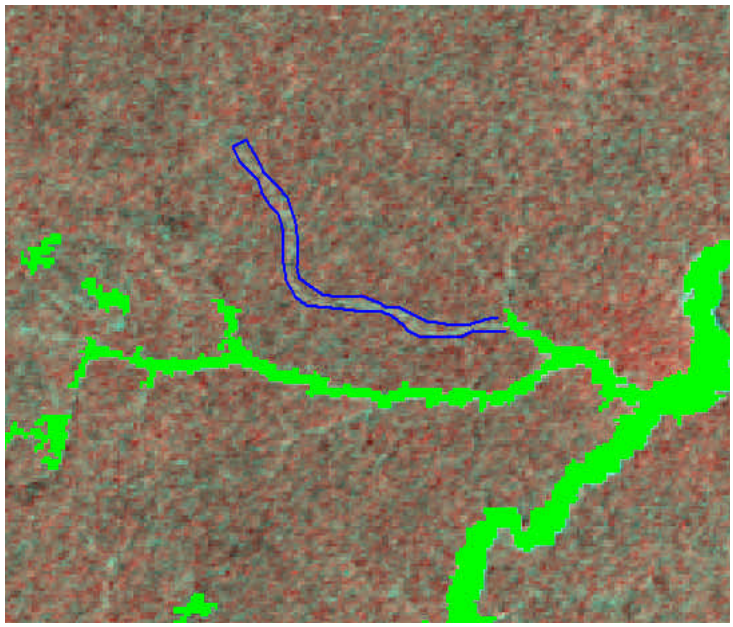

Figure 3 Outlining un-mapped flooded areas

(g) Quality control

At the end of editing, a SAR specialist who also has general familiarity with whole area performs the quality control. Georeferenced video data from some areas over the Amazon Basin is available and can be used as ground reference.

(h) Addition to the mosaic

After the quality control phase, the produced section is mosaicked with other sections.

4 RESULTS AND DISCUSSION

Optimizing segmentation time: As the image segmentation process demands significant computer processing time and the area to be mapped is extensive, 6 10^6 km^2 (each date image has approximately 600 Mbytes), the first tests were aimed to optimize the processing time of this phase. The segmentation time is directly related to the image set and image size being segmented. An approach to reduce the processing time was to test a series of products derived from the original data set as they related to the difference image (high water minus low water) and ratio image (high water/low water). Both products did not yield good results. Figure 4(a) shows the polygons for the difference image segmentation over the high water image. Some flooded regions were not outlined (light bluish). The band math applied to the data set decreased the class separability. Two adjacent regions belonging to distinct targets, visible in the original images, produced the same or almost the same digital count after the band operation.

Segmentation Thresholds: The next step was to define similarity and minimum area thresholds. For similarity, a tradeoff was inevitable; if it is too low, the growing process will generate over-segmented regions, with a large number of polygons and a large computing time; otherwise, polygons representing different cover type will be incorrectly merged together. After several experimental interactions applied to the images, the similarity and area thresholds were set to 6 and 50, respectively. They were set after a visual inspection secured that most of flooding areas were properly outlined. The minimum area was defined as a tradeoff between the mapping scale and the processing time. The 50 pixels value means that small regions, less than 50 pixels, will be merged with contiguous large regions, although they may be spectrally different. Figure 4(b) and (c) shows the result of different similarity thresholds. When a value of 10 was used as similarity, Figure 4(c), some flooded areas were not outlined. For the test site, segmentation resulted in 58,000 polygons. The segmentation software supplies the labeled image in two formats: a 32-bit raster image and a vector layer containing region polygons.

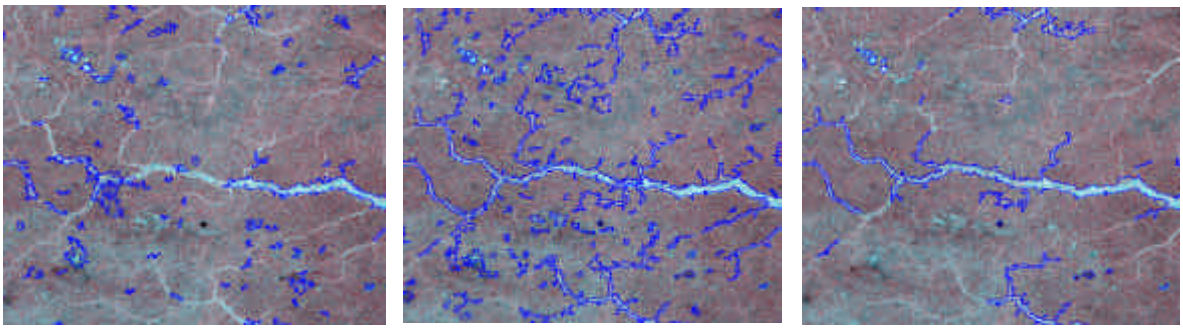

(a) (b) (c)

Figure 4 Segmentation results: a - Difference image (similarity= 6,area=50) b -Two dates images (similarity= 6,area=50) c - Two dates images(similarity=10,area=50)

Region-based classification: Two approaches were tested to merge thousands of labeled polygons from segmented image into three basic classes: open-water, non-flooded and flooded; supervised classification and unsupervised classification. For both classifications, the same feature extraction file was used.

First, a supervised region classifier based in the minimum Bhattacharrya distance (Richards, 1995) was applied. This classifier compares the statistics of the training polygons to the statistics of each polygon of the pre-segmented image.

This approach was partially successful for two reasons:

- It was not computationlly feasible to collect a number of samples accounting for extreme variability of the inundated area. As a consequence, some inundated areas were not classified. The large internal variance of the inundated areas can be confirmed from the result of unsupervised classification; where 36 of the 44 unsupervised classes were identified as flooded.
- When training polygon samples of non-flooded and open-water areas were selected instead of polygon samples of flooded areas, the classifier did not provide a good discrimination between flooded and non-flooded in some transition areas.

Several acceptance thresholds were tried. The results were later compared to those of the unsupervised classification approach.

For the unsupervised classifications, several acceptance thresholds were also tested. Figure 5 shows the classification results for different acceptance threshold values. Note that narrow water inundation channels that were classified as non-flooded for 90% acceptance threshold were accurately discriminated for 75% value. The discrimination between flooded and non-flooded was achieved by manipulating the acceptance threshold in transition areas. For the test site, the best acceptance threshold value was 75%.

The 44 clusters for the 75% acceptance threshold were classified as follows: 36 clusters of flooded areas, 6 of open-water and 2 of non-flooded. Figure 6 shows the results for the entire area.

5 CONCLUSIONS

The segmentation thresholds, applied to this section of mosaic (test site) seems to be adequate for other sections, but the classification thresholds must be assessed over each section, maybe because of differences in calibrations of distinct sections.

A detailed visual inspection of the results obtained from classification approaches shows that unsupervised classification provides a better discrimination of flooded and non-flooded areas, especially at the transition areas. On the other hand, the supervised classifier, using Bhattacharrya distance, seems less sensitive to the mosaic calibration problems.

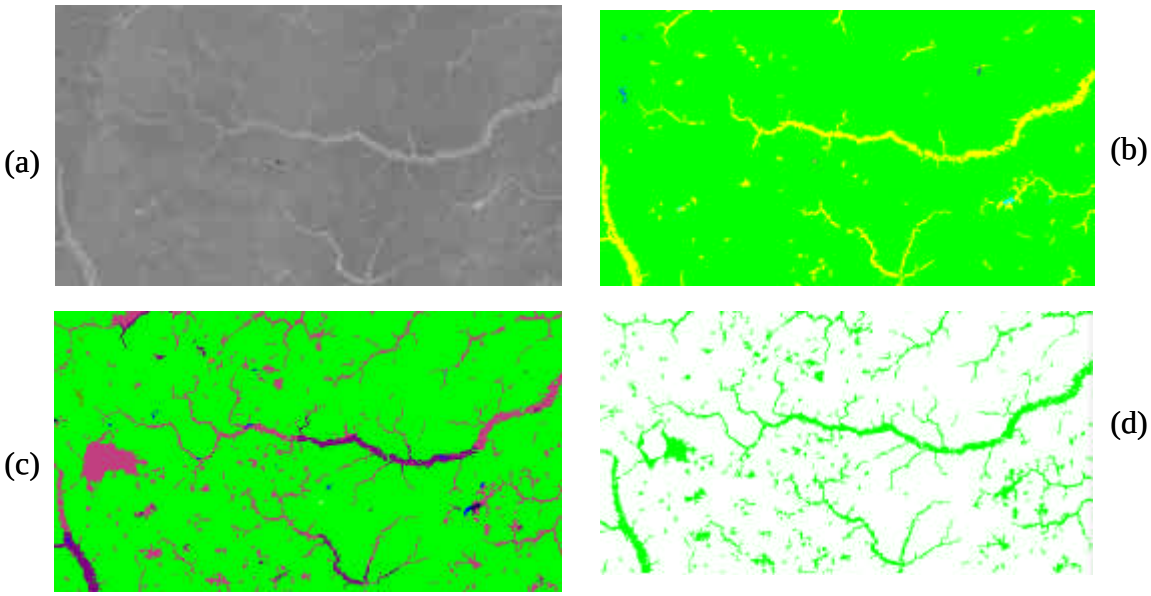

Figure 5 Classification results: a – High water Jers1 image b - Acceptance threshold 90% c - Acceptance threshold 75% d - Merge of unsupervised classes

An option tested during the development of this methodology that seems interesting, is to use the result of a supervised classification during the editing of the result of unsupervised classification, copying some areas that eventually were better discriminated. This procedure tends to reduce the editing time.

Results of this work demonstrated that region growing segmentation followed by a region clustering classification provides a viable approach to map wetlands from multi-date JERS1 images alone.

Using the described methodology, Hess et. al. 2003 has mapped a subset of the Amazon basin (08° S to 00° S, 72° W to 54° W), corresponding to the central Amazon region. An overall accuracy of 95% was obtained, assessed using high-resolution digital videography.

ACKNOWLEDGMENT

This research was supported by LBA-ECO investigation LC-07 and LC-11.The authors acknowledges JAXA and JPL for providing the data that made this research possible. We are also grateful to R. Cartaxo, J. d'Alge, Eymar L., and E. Kalil from INPE for providing information and assistance on SPRING Software.

REFERENCES

Armentano, (1991)T.V. Soils and Ecology: Tropical Wetlands. In Wetlands: A Threatened Landscape, edited by Michael Williams (Massachusetts: Basil Blackwell Ltd) 1991.

Batista, G.T.; Medeiros, J.C.; Mello, E.M.K.; Moreira, J.C.; Bins, L.S. (1994) A new approach for deforestation assessment. Proceedings of the International Symposium on Resource and Environmental Monitoring, Rio de Janeiro, Brazil. (Sao Paulo: INPE) pp. 170-174. 1994.

Bins, L.S.; Erthal, G.J.; Fonseca, L.M.G. (1992).Um metodo de classidicacao nao-supervisionada por regioes. Proceedings of Sixth Brazilian Symposium on Graphic Computation and Image Processing, Recife, Brazil. (Rio de Janeiro: Grafica Wagner) pp. 65-68. 1992.

Bins, L.S.; Fonseca, L.M.G.; Erthal, G.J.; Mitsuo II, F. (1996).Satellite Imagery Segmentation: a region Growing approach, VIII Simposio Brasileiro de Sensoriamento Remoto, Salvador, Bahia, Brazil, 1996.

Blake, D.R.; Rowland, F.S. (1986) Worldwide increase in tropospheric methane. Journal of Atmospheric Chemistry, 1978-1983. 4, 43-62, 1986.

Wetland Mapping: Manaus region

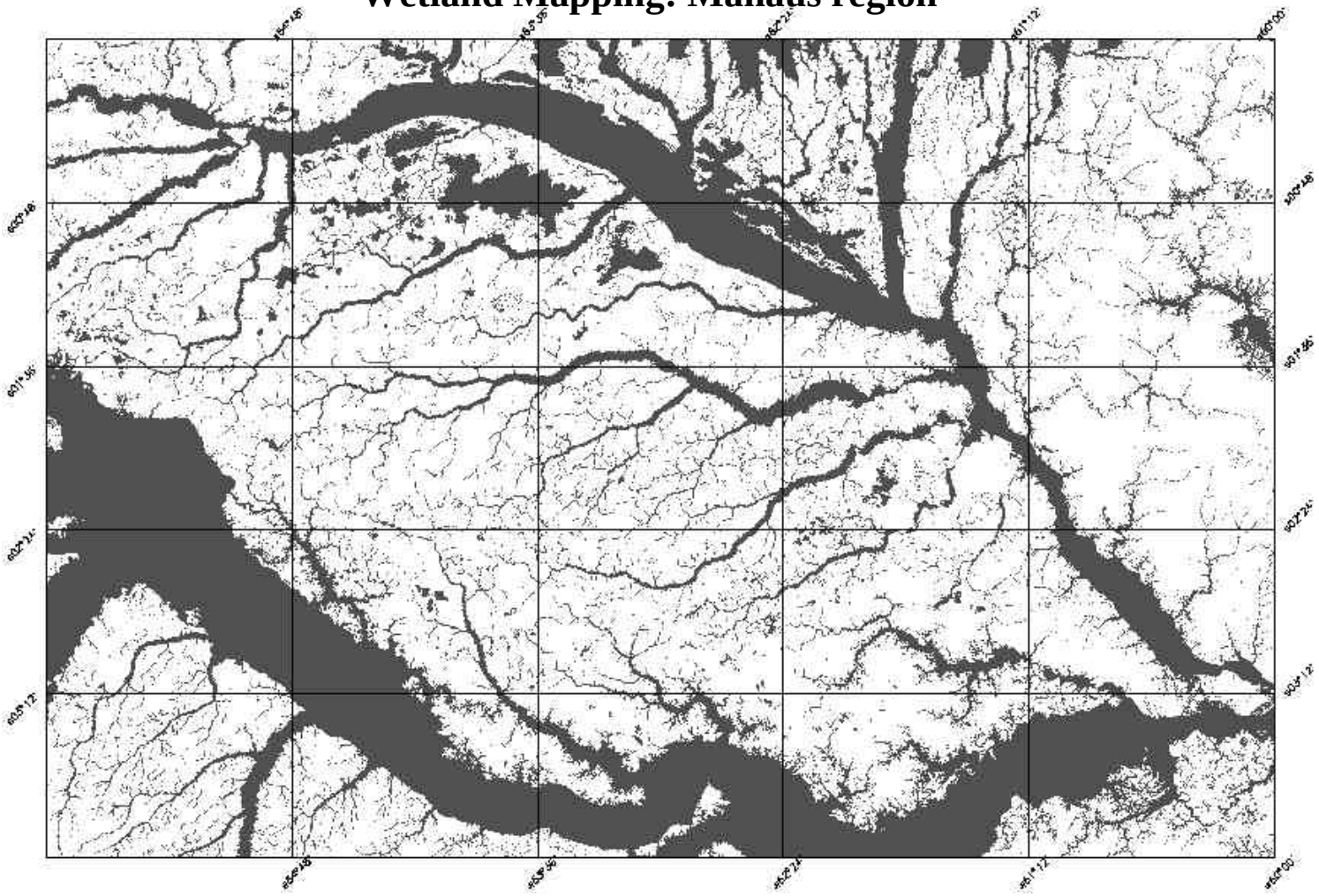

Flooded area: 92,400 Km^2 **No-flooded: 205,000 Km^2**

Camara, G.; Souza, R.C.M.; Freitas, U.M.; Garrido, J.C.P. (1996) SPRING: Integrating Remote Sensing and GIS by Object Oriented Data Modeling, Computer Graphics, 20(3), 1996.

Chapman, B., Siqueira, P. and Freeman, A., (2002). The JERS Amazon Multi-Season Mapping Study (JAMMS): observation strategies and data characteristics. Int. J. Remote Sens., 23: 1427–1446.

Costa, M.P.F.; Novo, E.M.L.M.; Ahern, F.; Mitsuo II, F.; Mantovani, J.E.; Ballester, M.V.; Pietsch, R.W. (1998) The Amazon Floodplain Through Radar Eyes: Lago Grande de Monte Alegre Case Study. Canadian Journal of Remote Sensing, 24: 339-349, 1998.

Freitas, C.C.; Correia, A.H.; Frery, A.C.; Sant' Anna, S.J.S.(1998) A system for multilook polarimetric SAR image statistical classification. Proceedings of the 2nd Latino-American Seminar on Radar on Remote Sensing held at Santos, Sao Paulo,Brazil, pp 141-148, 1998.

Goulding, M.; Smith, N.J.H., Mahar, D.J. (1995) "Floods of Fortune: Ecology and Economy Along the Amazon." Columbia University Press, New York. 193p. 1995.

Hess, L.L.; Melack, J.M.; Simonett, D. (1990) Radar Detection of Flooding Beneath the Forest Canopy: A Review. International Journal of Remote Sensing, 11 (7): 1313-1325, 1990.

Hess, L.L.; Melack, J.M.; Filoso, S.; Wang, Y.(1995) Delineation of inundated area and vegetation along the Amazon floodplain with the SIR-C synthetic aperture radar. IEEE Transactions on Geoscience and Remote Sensing, 33 (4): 896-904, July 1995

Hess, L.L.; Novo, M.L.M.; Valeriano, D.M.; Holts, J. W.; Melack, J.M.; (1998) Large-scale Vegetation Features of the Amazon Basin Visible on the JERS-1 Low-water Amazon Mosaic. IGARSS 98, Proceedings, Seatle, 6-10 July 1998,

Le Moigne, J.; Tilton, J.C. (1995)Refining Image segmentation by integration of edge and region data. IEEE Transactions on Geoscience and Remote Sensing, 33 (3): 605-615, May 1995

Lobo, A.; Chic, O.; Casterad, A. (1996) Classification of Mediterranean crops with multisensor data: per-pixel versus per-object statistics and image segmentation. International Journal of Remote Sensing, 17 (12): 2385-2400, 1996.

Lucca, E.V.D., Freitas, C.C.; Frery, A.C.; Sant' Anna, S.J.S. (1998) Comparison of SAR segmentation algorithms. Proceedings of the 2nd Latino-American Seminar on Radar on Remote Sensing held at Santos, Sao Paulo,Brazil, pp. 123-130, 1998.

Matthews, E.; Fung, I.(1987) Methane emission from natural wetlands: Global distribution, area, and environmental characteristics of sources Global Biogeochemical Cycles, 1, 61-86, 1987.

Mertes, L.A.K.; Novo, E.M.L.; Daniel, D.L.; Shimabukuro, Y.E.; Richey, J.E.; Krug, T. (1996) Classification of Rios Solimoes-Amazonas Wetlands through Application of Spectral Mixture Analysis to Landsat Thematic Mapper Data, VIII Simposio Brasileiro de Sensoriamento Remoto, Salvador-Brazil, 1996.

Novo, E.M.L.M.; Leite, F.A.; Avila, J.; Ballester, M.V.; Melack, J.M. (1997) Assessment of Amazin Floodplain Habitats Using TM/Landsat Data. Ciencia e Cultura, 49(4): 280-284, 1997.

Oliver, C.; Quegan, S. (1998)Understanding synthetic aperture radar images. Boston: Artech House, 1998.

Pal, N.R.; Pal, S.K. (1993) A review on image segmentation techniques. Pattern Recognition, 26(9): 1277-1294,

Richards, J. A. (1995)Remote Sensing Digital Image Analysis. An Introduction. New York, Springer-Verlag, 1995.

Richey, J. E.; Victoria, R. L.; Salati, E.; Forsberg, B.R. (1991) The biogeochemistry of a major river system: the Amazon case study. In Biogeochemistry of Major World Rivers, edited by E.T. Degens, S. Kempe and J.E. Richey(New York: John Wiley), pp 57-74. 1991.

Sant' Anna, S.J.S.; Freitas, C.C.; Renno. C.D. (1998) A system for multilook polarimetric SAR image statistical classification. Proceedings of the 2nd Latino-American Seminar on Radar on Remote Sensing held at Santos, Sao Paulo,Brazil, pp 99-106, 1998.

Shimabukuro, Y.E.; Batista, G.T.; Mello, E.M.K.; Moreira, J.C.; Duarte, V. (1998) Using shade fraction image segmentation to evaluate deforestation Landsat Thematic Mapper images of the Amazon Region. International Journal of Remote Sensing, 19(3): 535-541, 1998.

Sioli, H. (1984) The Amazon and its main affluents: Hydrography, Morphology of river courses, and river types. In Amazon: Limnology and Landscape Ecology of a Mighty tropical River and its Basin, edited by H. Sioli (Dordrecht: W. Junk), pp 127-166, 1984.

Sioli, H. (1968)Hydrochemistry and geology in the Brazilian Amazon region. Amazoniana 1: pp 267-277, 1968.

Williams, M. (1991)Understanding Wetlands. In Wetlands: A Threatened Landscape, edited by Michael Williams (Massachusetts: Basil Blackwell Ltd) 1991